Phase stability and magnetism in NiPt and NiPd alloys

2004 J. Phys.: Condens. Matter 16 5791

(http://iopscience.iop.org/0953-8984/16/32/015)

INSTITUTE OF PHYSICS PUBLISHING JOURNAL OF PHYSICS: CONDENSED MATTER

J. Phys.: Condens. Matter **16** (2004) 5791–5802 PII: S0953-8984(04)78879-7

Phase stability and magnetism in NiPt and NiPd alloys

Durga Paudyal and Abhijit Mookerjee

S N Bose National Centre for Basic Sciences, JD Block, Sector 3, Salt Lake City, Kolkata 700098, India

E-mail: dpaudyal@bose.res.in and abhijit@bose.res.in

Received 2 April 2004
Published 30 July 2004
Online at stacks.iop.org/JPhysCM/16/5791
doi:10.1088/0953-8984/16/32/015

Abstract

We show that the differences in stability of 3d–5d NiPt and 3d–4d NiPd alloys arise mainly due to relativistic corrections. The magnetic properties of disordered NiPd and NiPt alloys also differ due to these corrections, which lead to increase in the separation between the s–d bands of 5d elements in these alloys. For the magnetic case we also analyse the results in terms of splitting of majority and minority spin d band centres of the 3d elements. We further examine the effect of relativistic corrections to the pair energies and order–disorder transition temperatures in these alloys. The magnetic moments and Curie temperatures have also been studied along with the short range ordering/segregation effects in NiPt/NiPd alloys.

1. Introduction

It is well known at the level of standard chemistry that the main chemical difference between pairs of 4d and 5d transition elements is the relativistic contraction of the valence s and p states relative to the d and f states. Recently, Wang and Zunger [1] studied ordered 3d–5d (NiPt) and 3d–4d (NiPd) alloys and pointed out the effect of relativistic corrections in the formation energies in these alloys. In this communication we shall provide a quantitative, electronic structure analysis of these corrections in both the ordered as well as the disordered phases of NiPt and NiPd alloys including magnetism as well, and demonstrate its consequences for phase stability. We shall show, via a first-principles calculation, that in binary alloys of the late 3d–5d intermetallics, the 3d–5d coupling is dominant. This effect results from the relativistic upshift of the 5d band, which brings it closer to the 3d band of the other element, significantly enhancing the 3d–5d hybridization. In addition, the relativistic s orbital contraction significantly reduces the lattice constant of the 5d element, thus lowering the size mismatch with the 3d element. This reduces the strain energy associated with packing 3d and 5d atoms of dissimilar sizes into a given lattice. Both the enhanced d–d hybridization and the reduced packing strain are larger in 3d–5d intermetallics than in 3d–4d ones. This explains why the 3d–5d alloys

(NiPt in this case) have negative formation energies and thus form stable ordered alloys, whereas the analogous isovalent 3d–4d alloys (NiPd), made of elements from the same columns in the periodic table, have positive formation energies and thus either phase separate or remain mostly in disordered phases. Simple arguments, such as ones based on atomic size mismatch or electronegativity differences, do not explain these two different behaviours. The constituent elements in the stable NiPt alloys have larger atomic size mismatch than the unstable NiPd.

Our calculation of pair energies shows that the inclusion of relativistic effects in the electronic structure calculation is often important for getting the correct ordering behaviour seen experimentally. It is known experimentally that NiPt is ordered at low temperatures while NiPd remains disordered but with a tendency toward short ranged clustering. To obtain the correct ordering tendency for NiPt we need to carry out scalar relativistic calculations. For NiPd we have to carry out calculations on the disordered alloy with short ranged clustering effects included, so as to give the correct magnetic moment per atom.

From experiments, the difference in magnetic properties of disordered NiPd and NiPt alloys does not seem to be obvious, as Pd and Pt have the same number of valence electrons. Earlier works [2–4] on the magnetic properties of NiPd and NiPt alloys used parametrized local environment models to describe the magnetism in NiPd and NiPt alloys. These models incorporated the changes induced due to the chemical environment as well as the magnetic environment. The present study is intended to improve our understanding of the factors which led to differences in the magnetic properties of disordered NiPd and NiPt alloys and to determine the effect of chemical, as well as magnetic, environments from a first-principles approach.

In an earlier communication [5] we have pointed out that the environmental effect is important in NiPt alloys. The environmental effect is intrinsically a many-site problem. An approximate treatment of correlation effects between a site and its neighbours has been carried out within a single-site coherent potential approximation by Staunton *et al* [6]. However, any approximation that explicitly involves more than one site is expected to give a better qualitative and quantitative picture. The recently developed itinerant cluster approximation of Ghosh *et al* [7] is one example. So far it has been applied only to phonons. The augmented space recursion (ASR) [8] used in our work is another. Both these techniques are based upon the augmented space theorem [9]. The reason for emphasizing environment effects for alloys of Ni with non-magnetic metals (such as Pt and Pd) is that the local magnetic moment of Ni in such an alloy is strongly dependent on its environment. In a fcc lattice, a Ni atom has to be surrounded by at least six other Ni atoms; otherwise no local moment can be sustained on it. In this paper we find that in NiPd short ranged segregation occurs in an otherwise disordered alloy. This actually enhances ferromagnetic behaviour on a par with the experimental predictions.

The differences in the magnetic properties of NiPd and NiPt alloys are also dictated by the electronic structure of 4d Pd and 5d Pt atoms and the subsequent hybridization of these states with the d states of Ni atoms. Since relativistic corrections are more important for heavier elements, the differences in electronic structure of Pd and Pt atoms are mainly due to relativistic effects.

2. Theoretical and computational methods

For ordered structures we have performed total energy density functional calculations. The Kohn–Sham equations were solved in the local density approximation (LDA) with von Barth–Hedin (vBH) [10] exchange correlations. The calculations were performed in the basis of tight binding linear muffin-tin orbitals in the atomic sphere approximation (TB-LMTO-ASA) [11–14] including combined corrections. Two sets of calculations have been performed: one scalar relativistic through inclusion of mass–velocity and Darwin correction terms and another

without. The k-space integration was carried out with a $32 \times 32 \times 32$ mesh resulting in 2601 k-points for tetragonal primitive structures in the irreducible part of the corresponding Brillouin zone. The convergence of the total energies with respect to k-points has been checked.

As we know, when the alloy is formed the elemental solids are deformed from their equilibrium lattice constants (a_{A}^0, a_{B}^0) to the lattice constants (a) of the final alloy. Therefore, in the alloy formation there are two kinds of formation energies. One is elastic formation energy which is given as

$$\Delta H_{\mathrm{elast}} = x[E_{\mathrm{A}}(a) - E_{\mathrm{A}}(a_{\mathrm{A}}^0)] + (1-x)[E_{\mathrm{B}}(a) - E_{\mathrm{B}}(a_{\mathrm{B}}^0)]$$

and another is chemical formation energy which is given as

$$\Delta H_{\mathrm{chem}} = E(\mathrm{A}_x\mathrm{B}_{1-x}; a) - xE_{\mathrm{A}}(a) - (1-x)E_{\mathrm{B}}(a)$$

where x is the concentration of one of the constituents.

The sum of these formation energies is the conventional alloy formation energy:

$$\Delta H = \Delta H_{\mathrm{elast}} + \Delta H_{\mathrm{chem}}. \tag{1}$$

For stability arguments, we start from a completely disordered alloy. Each site R has an occupation variable n_R associated with it. For a homogeneous perfect disorder $\langle n_R \rangle = x$, where x is the concentration of one of the components of the alloy. In this homogeneously disordered system we now introduce fluctuations in the occupation variable at each site: $\delta x_R = n_R - x$. Expanding the total energy in this new configuration about the energy of the perfectly disordered state we get

$$E(x) = E^{(0)} + \sum_{R=1}^{N} E_R^{(1)} \delta x_R + \sum_{RR'=1}^{N} E_{RR'}^{(2)} \delta x_R \delta x_{R'} + \cdots. \tag{2}$$

The coefficients $E^{(0)}$, $E_R^{(1)}$ ... are the effective renormalized cluster interactions. $E^{(0)}$ is the energy of the averaged disordered medium. The renormalized *pair interactions* $E_{RR'}^{(2)}$ express the correlation between concentration fluctuations at two sites and are the dominant quantities for the analysis of phase stability. In the series expansion, we will retain terms only up to pair interactions. Higher order interactions may be included for a more accurate and complete description.

The total energy of a solid may be separated into two terms: a one-electron band contribution E_{BS} and the electrostatic contribution E_{ES}. The renormalized cluster interactions defined in (2) should, in principle, include both E_{BS} and E_{ES} contributions. Since the renormalized cluster interactions involve the difference of cluster energies, it is usually assumed that the electrostatic terms cancel out and only the band structure contribution is important. Such an assumption, which is not rigorously true, has been shown to be approximately valid in a number of alloy systems [15]. Considering only band structure contributions, it is easy to see that the effective pair interactions may be written as

$$E_{RR'}^{(2)} = E_{RR'}^{\mathrm{AA}} + E_{RR'}^{\mathrm{BB}} - E_{RR'}^{\mathrm{AB}} - E_{RR'}^{\mathrm{BA}}. \tag{3}$$

We have computed these pair energies using augmented space recursion with the TB-LMTO Hamiltonian coupled with orbital peeling which allows us to compute configuration averaged pair potentials directly, without resorting to calculations involving small differences of large total energies. The details of this method are given in our previous paper [16] and the references therein.

For the calculation of the order–disorder transition temperature we have used Khachaturian's concentration wave approach in which the stability of a solid solution with

respect to a small concentration wave of given wavevector $\vec{k}$ is guaranteed as long as $k_B T + V(\vec{k})c(1-c) > 0$. Instability of the disordered state sets in when

$$k_B T^i + V(\vec{k})c(1-c) = 0. \tag{4}$$

T^i is the instability temperature corresponding to a given concentration wave disturbance. $V(\vec{k})$ is the Fourier transform of pair energies and c is the concentration of one of the constituent atoms. The details are given in our previous paper [16] and references therein.

The antiphase boundary energies between $L1_0$ and $L1_2$ structures and their corresponding superstructures A_2B_2 and $D0_{22}$ [17] are

$$\xi = -V_2 + 4V_3 - 4V_4; \tag{5}$$

for $\xi > 0$, $L1_2$ and $L1_0$ are the stable structures at concentration 25% and 50%, while for $\xi < 0$, the stable superstructures are DO_{22} and A_2B_2.

Our magnetic calculations are based on the generalized ASR technique [5, 18–22]. The Hamiltonian in the TB-LMTO minimal basis is sparse and therefore suitable for treatment with the recursion method introduced by Haydock *et al* [23]. The ASR allows us to calculate the configuration averaged Green functions. It does so by augmenting the Hilbert space spanned by the TB-LMTO basis with the configuration space of the random Hamiltonian parameters. The configuration average is expressed *exactly* as a matrix element in the augmented space. A generalized form of this methodology is capable of taking into account the effect of short range order. Details are given in our previous paper [5] and references therein.

For the treatment of the Madelung potential, we follow the procedure suggested by Kudrnovský *et al* [24] and use an extension of the procedure proposed by Andersen *et al* [11]. We choose the atomic sphere radii of the components in such a way that they preserve the total volume on average and the individual atomic spheres are almost charge neutral. This ensures that total charge is conserved, but each atomic sphere carries no excess charge. In doing so, one needs to be careful about the sphere overlap which should be under a certain limit so as not to violate the atomic sphere approximation.

To calculate the Curie temperature T_C we have used the Mohn–Wohlfarth (MW) procedure [25]:

$$\left(\frac{T_C}{T_S}\right)^2 + \frac{T_C}{T_{SF}} - 1 = 0$$

where T_S is the Stoner temperature calculated from the relation

$$\langle I(E_F)\rangle \int_{-\infty}^{\infty} \mathrm{d}E\, N(E)\left(\frac{\partial f}{\partial E}\right) = 1.$$

$\langle I(E_F)\rangle$ is the concentration averaged Stoner parameter, $N(E)$ is the density of states per atom per spin of the paramagnetic state [26] and $f(E)$ is the Fermi distribution function. The spin fluctuation temperature T_{SF} is given by

$$T_{SF} = \frac{m^2}{10 k_B \langle \chi_0 \rangle}.$$

$\langle \chi_0 \rangle$ is the concentration weighted, exchange enhanced spin susceptibility at equilibrium and m is the averaged magnetic moment per atom. χ_0 is calculated using the relation given by Mohn [25] and Gersdorf [27]:

$$\chi_0^{-1} = \frac{1}{2\mu_B^2}\left(\frac{1}{2N^{\uparrow}(E_F)} + \frac{1}{2N^{\downarrow}(E_F)} - I\right).$$

$N^{\uparrow}(E_F)$ and $N^{\downarrow}(E_F)$ are the spin-up and spin-down partial densities of states per atom at the Fermi level for each species in the alloy.

Table 1. Formation energies in mRyd/atom and lattice parameters in au. The values shown in brackets are the ones without relativistic corrections.

Alloy system	ΔH_{form}	$\Delta H_{\text{elastic}}$	$\Delta H_{\text{chemical}}$	a	c/a
NiPd (this work)	3.54 (5.38)	17.05 (18.13)	−13.51 (−12.75)	7.10	0.923
Wang and Zunger [1]	3.63 (6.22)	19.83 (21.05)	−16.20 (−14.83)	7.11	0.924
NiPt (this work)	−9.17 (4.44)	22.22 (31.48)	−31.39 (−27.04)	7.16	0.927
Wang and Zunger [1]	−6.26 (8.17)	29.74 (40.38)	−36.00 (−32.21)	7.175	0.926

In these calculations one also needs to be very careful about the convergence of our procedure. Errors can arise in the augmented space recursion because one can carry out only a finite number of recursion steps and then terminate the continued fraction using available terminators. We ensure that the recursion is carried out for a sufficient number of steps so that the errors in Fermi energy, moments of the density of states and magnetic moment remain within prescribed windows.

The formulation of the augmented space recursion used for the calculation in the present paper is the energy dependent augmented space recursion in which the disordered Hamiltonian with diagonal as well as off-diagonal disorder is recast into an energy dependent Hamiltonian having only diagonal disorder. We have chosen a few seed points across the energy spectrum uniformly, carried out recursion on those points and spline fitted the coefficients of recursion throughout the whole spectrum. This enabled us to carry out a large number of recursion steps since the configuration space grows significantly less quickly for diagonal as compared with off-diagonal disorder. Convergence of physical quantities with recursion steps was discussed in detail earlier by Ghosh *et al* [28, 29].

3. Results and discussion

3.1. Calculations on ordered alloys

3.1.1. Formation energies. In table 1, we show the calculated formation energies of the $L1_0$ structure of NiPd and NiPt alloys calculated relativistically (including mass–velocity and Darwin corrections but without spin–orbit couplings) as well as non-relativistically. The table shows the lattice parameters calculated by minimizing the total energy. The parameter a and the ratio c/a are in very good agreement with those found by Wang and Zunger [1] (see table 1). The relativistically calculated formation energies (in mRyd/atom) are 3.54 and −9.17 for NiPd and NiPt. We see a clear ordered alloy formation trend for NiPt as contrasted with the disordering trend of NiPd. To gain better insight into those trends, we have decomposed the total formation energies into chemical formation energies and elastic formation energies. The elastic energy of formation is the energy needed to deform the elemental solids A and B from their respective equilibrium lattice constants and to the lattice constants of the final AB alloy. Since a deformation of equilibrium structures is involved, the chemical energy of formation is simply the difference between the (fully relaxed) total energy of the alloy and the energies of the deformed constituents. In general the elastic formation energy is positive and the chemical formation energy is negative. The sum gives the conventional definition of alloy formation energy and the system is stable only if this formation energy is negative. This clearly shows that a lower volume deformation energy of the constituents enhances the (negative) chemical formation energy giving rise to the possibility of forming a stable ordered alloy.

Table 1, shows that the relativistic effect significantly reduces the elastic energy of formation of 3d–5d alloys (e.g. from 31.48 to 22.22 mRyd/atom for NiPt). This effect is

Table 2. Band centres (C) mRyd/atom. The values shown in brackets are the ones without relativistic corrections.

Alloy system	Site (A/B)	s orbital	p orbital	d orbital
NiPd	Ni	−359.0 (−343.6)	676.3 (650.5)	−217.1 (−228.0)
	Pd	−317.6 (−240.8)	746.2 (763.1)	−321.9 (−335.0)
NiPt	Ni	−349.4 (−347.2)	707.0 (641.4)	−210.5 (−227.9)
	Pt	−524.0 (−283.8)	642.1 (694.0)	−324.8 (−366.3)

Table 3. Hopping integrals (Δ) mRyd/atom. The values shown in brackets are the ones without relativistic corrections.

Alloy system	Site (A/B)	s orbital	p orbital	d orbital
NiPd	Ni	176.1 (172.6)	155.9 (152.7)	9.9 (9.4)
	Pd	182.3 (184.8)	186.7 (184.3)	22.7 (21.1)
NiPt	Ni	177.6 (167.6)	151.5 (142.8)	9.4 (8.4)
	Pt	163.6 (175.0)	186.4 (183.4)	29.8 (25.5)

much smaller in the 3d–4d systems (e.g. from 18.13 to 17.05 mRyd/atom in NiPd). The reason for this can also be appreciated by inspecting the non-relativistically and relativistically calculated equilibrium lattice constants of the fcc elements as already shown by Wang and Zunger [1].

In addition to the reduction in the (positive) elastic energy of formation, table 1 also shows that relativistic corrections enhance the (negative) chemical energy of formation (e.g. from −27.04 to −31.39 mRyd/atom for NiPt). This effect is much smaller in 3d–4d alloys (e.g. from −12.75 to −13.51 mRyd/atom for NiPd). There are two effects that explain this relativistic chemical stabilization. First the relativistic raising of the energy of the 5d state reduces the 3d–5d energy difference and thus improve the 3d–5d bonding; second the relativistic lowering of the s bands and raising of the d band leads to an increased occupation of the bonding s bands and a decreased occupation of the antibonding d band. These effects can be appreciated by observing the band centres shown in table 2; we can see that the 5d and 3d bands are closer to each other in the relativistic limit than in the non-relativistic limit and play an important role in the formation energies of these alloys. From table 3, it is seen that the difference between the hopping integrals for 3d and 5d is higher than the difference between the hopping integrals for 3d and 4d in the relativistic case, which is the signature of higher overlap and hence stability in NiPt alloys with relativistic corrections. The d–d interaction from different sublattices in late d alloys plays a key role. Relativity results in the raising of the energy of the 5d band (bringing the 5d band closer to the 3d band) and in a large charge transfer from the antibonding edge of the 5d band to the bonding 6s, p bands, thus enhancing the chemical stability of the 3d–5d alloys.

Although our calculations were based on the TB-LMTO and the von Barth–Hedin exchange correlation, while those of Wang and Zunger [1] were based upon the full potential linearized augmented plane wave method with exchange–correlation functional of Ceperley and Alder parametrized by Perdew and Zunger [1], the differences of the various energy terms are no more than a few mRyd/atom, which is within the error window of our methodology.

3.1.2. Separation between s and d band centres. It is seen that phase stability in 3d–5d alloys is brought about by relativity through its effect on heavier atoms. We know that the dominant effect of relativity is to lower the s potential. From table 2 it is clearly seen that the energy band centre of Pt in NiPt is lower in the relativistic case than in the non-relativistic case. The

Table 4. Pair energies in mRyd/atom. The values shown in brackets are the ones without relativistic corrections.

Alloy system	v_1	v_2	v_3	v_4
NiPd	5.16 (4.56)	0.02 (−0.16)	0.05 (0.09)	0.07 (0.09)
NiPt	10.08 (10.11)	0.10 (0.13)	0.01 (0.25)	−0.24 (0.17)

lowering of the s potential causes (i) the s wavefunction to contract leading to a contraction of the lattice and (ii) increased s–d hybridization which results in electron transfer from d to s. We see that the change in s–d separation is greater in Pt in NiPt alloys than in Pd in NiPd. The s–d separation for Pd in NiPd alloy changes from 94.3 to 4.3 mRyd, whereas for Pt in NiPt alloy, it changes from 82.5 to −199.2 mRyd. The contraction of the s wavefunction of Pt and the subsequent s–d hybridization must be responsible for the reduction in the size mismatch and hence reduces the strain in NiPt alloys giving rise to the stable structures.

3.2. Calculations for disordered alloys

3.2.1. Effective pair energies. In table 4, we show the effective pair energies up to fourth-nearest neighbours in 3d–4d NiPd and 3d–5d NiPt alloys.

The first-nearest neighbour pair interaction in NiPt shows ordering behaviour. Indeed, with the relativistic correction, the antiphase boundary energy indicates a stable ordered $L1_0$ low temperature phase. The formation energy of the $L1_0$ phase is negative, confirming stability. However, the formation energy in NiPt with the non-relativistic calculation turns out to be positive, which shows the necessity of including relativistic corrections in the electronic structure calculations.

For NiPd we have a problem. Although the positive nearest neighbour pair interaction indicates an ordering tendency, even with relativistic correction the antiphase boundary energy and the formation energies indicate that the ordered structure is not stable at low temperatures. This remains true even if we include magnetic effects in the pair interaction. This alloy remains disordered at low temperatures. However, whether this is because of the fact that at low temperatures the atomic mobilities are too low for ordering to proceed quickly (as in AgPd, for example) one cannot say with certainty.

3.2.2. Order–disorder transition temperatures. Using these pair interactions obtained by us, we have calculated the instability temperatures in NiPt with relativistic corrections. For the entropy part we have taken a simple mean-field Bragg–Williams expression. The calculated instability temperature in NiPt comes out as 1683 K, which is higher than the experimental estimate which was discussed in great detail in our previous paper [16]. The Bragg–Williams expression tends to overestimate the transition temperature, consistent with our results.

Our calculations (with relativistic corrections) indicate that the order–disorder transition takes place in NiPd at around (812 K), slightly above the non-relativistic one (743 K). Although first-principles calculation indicates there should be a disorder–order transition, low atomic mobility prevents a transition to order in this alloy system. This is similar to the AgPd alloy system case. Since there is no experimental evidence of an order–disorder transition in this system, we only comment that this system mainly tends to remain in a disordered phase. Looking at the high value (457 K) of the experimental Curie temperature we can argue that, there, magnetism should have an effect on the phase stability of the NiPd system, reducing the value of the order–disorder transition temperature. Our calculation including magnetism did indeed lower the order–disorder transition temperature.

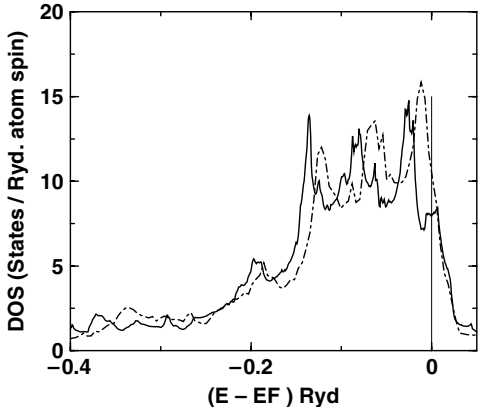

Figure 1. The paramagnetic density of states for d bands of Ni in ordered NiPd (dotted curves) and NiPt alloys (solid curves).

3.3. Magnetic calculations for NiPd and NiPt alloys

In figure 1, we show the paramagnetic density of states for d bands of Ni in ordered NiPd and NiPt alloys. It is seen that the d band of Ni is narrow in NiPd in comparison to NiPt, which suggests that Ni in NiPd has a higher magnetic moment than Ni in NiPt alloys.

To understand quantitatively the differences in magnetic properties of these two systems, we have studied the separation between the majority and minority spin d band centres, the separation between s and d band centres and the spin polarized density of states in these NiPd and NiPt alloys.

3.3.1. Separation between majority and minority spin d band centres. The changes in the magnetic moments due to relativistic effects can be explained by examining the separation between majority spin and minority spin d band centres of Ni ($\Delta C^{\mathrm{Ni}}_{\mathrm{d}\uparrow-\mathrm{d}\downarrow}$) in NiPd and NiPt alloys.

We observe that the exchange-induced splitting of the d band is higher in Ni–Pd alloys for calculations done with and without relativistic corrections. The higher splitting leads to an increase in the local magnetic moment at the Ni site. It is interesting to note that the inclusion of relativistic corrections produces no net change in the exchange-induced splitting at the Ni site in NiPd. In NiPd, due to these corrections, the separation between d band centres changes from 55.4 to 57.3 mRyd/atom, giving rise to 0.75–0.76 μ_{B}/atom. On the other hand, in NiPt alloy we find that relativity substantially reduces the exchange-induced splitting at the Ni site, leading to a decrease in the local magnetic moment of Ni. In NiPt the separation between d band centres reduces from 46.0 to 21.9 mRyd/atom due to relativity giving rise to the corresponding reduction in the local magnetic moment from 0.59 to 0.30 μ_{B}/atom.

3.3.2. Separation between s and d band centres. It is clear that the differences in magnetic properties of Ni–Pd and Ni–Pt alloys are brought about by relativity through its effect on Pd and Pt atoms. We know that the dominant effect of relativity is to lower the s potential. The lowering of the s potential causes (i) the s wavefunction to contract leading to a contraction of the lattice and (ii) increased s–d hybridization which results in electron transfer from d to s. We see that the change in the s–d separation is greater in Pt than in Pd. The s–d separation for Pd in NiPd alloy changes from +59.0 to 7.6 mRyd, whereas for Pt in NiPt alloy, it changes from

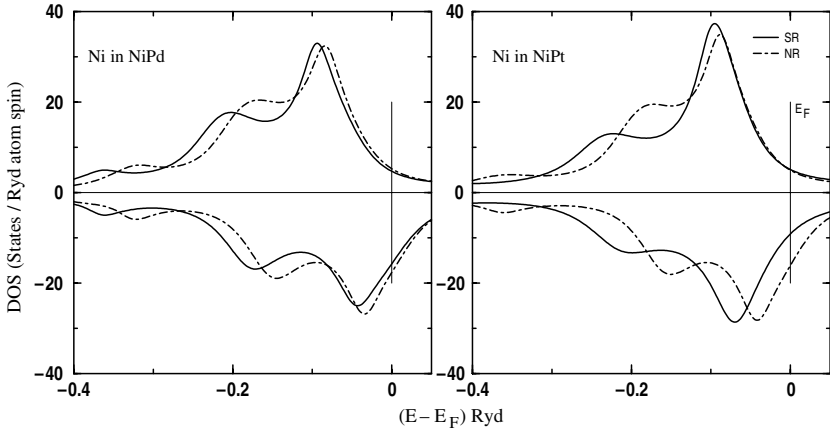

Figure 2. The spin polarized densities of states of Ni, calculated non-relativistically (NR) and scalar relativistically (SR), in disordered NiPd and NiPt alloys.

+84.0 to −199.1 mRyd. Thus the contraction of the s wavefunction of Pt and the subsequent s–d hybridization must be responsible for reducing the local magnetic moment at the Ni site in NiPt.

3.3.3. Spin polarized densities of states. In figure 2 we show the spin polarized DOS at the Ni site for disordered NiPd and NiPt alloys calculated with and without relativistic corrections. Since relativity is more important for NiPt than for NiPd, its effect on the DOS at the Ni site in NiPt is clearly seen. From the figure we see the substantial differences in density of electrons at the Fermi level between the non-relativistic and scalar relativistic cases for NiPt alloy, but there are negligible differences in the case of NiPd.

3.3.4. Magnetic moments. From table 5 it is seen that magnetic moments calculated with and without relativistic corrections are similar in ordered as well as disordered NiPd alloys. However, the calculated average as well as local magnetic moments are quite different, for ordered as well as disordered NiPt alloys, in the cases with and without relativistic corrections. We find that the inclusion of relativity leads to a decrease in the magnetic moment at the Ni site by 0.29 μ_B/atom in the NiPt alloy system. Our theoretically calculated disordered magnetic moment of NiPt with relativistic correction agrees with experimental estimates. Experimentally, NiPt has the effect of atomic short range order. With the inclusion of short range order effects we could get the magnetic moment of Ni even closer to the experimental value. The short range order effect in the magnetism of the NiPt system is more important for the higher concentrations of Pt (55% and 57%) which we described in our previous paper [5]. The calculated magnetic moment of Ni in NiPd alloy is very low (0.76 mRyd/atom) in comparison to the diffuse scattering experiment result (1.02 mRyd/atom). This disagreement led us to suspect an effect of short range order on the magnetism of NiPd alloy. In order to check for a possible short range order effect, we have checked the variation of the total energy as a function of the short range order parameter and found that the total energy decreases as the short range order parameter goes from negative (ordering side) to positive (segregation side), confirming this system to be a segregating system. We then checked the variation of the magnetic moments as a function of the SRO parameter and found that the magnetic moment of Ni increases by an appreciable fraction. The moment of Pd decreases. This gives rise to the increase of the

Table 5. Calculated local and average magnetic moments in μ_B/atom of NiPd and NiPt alloys. SRO and SRS denote short range order and short range segregation.

NiPd alloy				
Method	System	Ni site	Pd site	Average
TB-LMTO	Ordered (SR)	0.70	0.29	0.50
	Ordered (NR)	0.70	0.26	0.48
ASR	Disordered (SR)	0.76	0.31	0.54
	Disordered (NR)	0.75	0.28	0.51
	Disordered (SR) with SRS	0.90	0.27	0.59
Expt [3]	Disordered	1.02	0.17	0.60
NiPt alloy				
Method	System	Ni site	Pt site	Average
TB-LMTO	Ordered (SR)	0.31	0.16	0.23
	Ordered (NR)	0.65	0.22	0.44
ASR	Disordered (SR)	0.30	0.11	0.20
	Disordered (NR)	0.59	0.21	0.40
	Disordered (SR) with SRO	0.27	0.14	0.21
Expt [2]	Disordered	0.28	0.17	0.22

average magnetic moment. Calculated magnetic moments (0.90, 0.27 and 0.59 μ_B/atom for Ni, Pd and the average in NiPd) including the effect of segregation in this system agree closely with the corresponding experimental values (1.02, 0.17 and 0.59 μ_B/atom for Ni, Pd and the average).

The average magnetic moments are higher for the disordered case, compared to the ordered case, in NiPd. This is because of the tendency in NiPd toward disordering or clustering, which allows Ni to be favourably surrounded by Ni, strengthening its local magnetic moment. In NiPt, the tendency is toward ordering or Ni being favourably surrounded by Pt atoms, which lowers the fragile local magnetic moment of Ni.

To our knowledge there is no experimental measurement available for local as well as average magnetic moments in ordered NiPt and NiPd alloys. The experimental measurements for local as well as average magnetic moments by Parra *et al* [2] for NiPt and by Cable *et al* [3] for NiPd were for disordered alloys.

3.3.5. Curie temperature. We have applied the Mohn–Wohlfarth model to calculate the Curie temperature, as explained in the theoretical and computational details. Our Curie temperature calculation for NiPt with the relativistic correction (76 K) shows closer agreement with the experimental value (100 K). In contrast, the Curie temperature without relativistic correction in the electronic structure calculation turns out (199 K) to be higher than the experimental estimate. This again supports the assertion that the relativistic effect plays a significant role in the correct estimation of magnetic transitions as well as magnetic moments. In the NiPd system the calculated Curie temperatures with (245 K) and without relativistic correction (199 K) do not differ much, as in the case of magnetic moments as explained above. The slightly higher value in the relativistic case may be due to the slightly higher (57.3 mRyd/atom) value of the difference in d band centres than in the non-relativistic case (55.4 mRyd/atom). These values of Curie temperatures with and without relativistic corrections do not actually match with the experimental value (457 K). As we have explained above, in the connection of magnetic

moments there is a possibility of enhancement of the magnetism due to the segregation tendency of this system. Our calculation taking into account this segregation effect through a short range order parameter does indeed show a Curie temperature (345 K) closer to the experimental estimate. Therefore, one can argue that in the NiPd alloy system the atomic segregation tendency leads to a strong enhancement in the magnetism.

4. Conclusions

Our calculation for formation energies shows that NiPt systems are stabilized by the inclusion of relativistic effects. These effects ensure larger s–d hybridization by lowering s orbitals and raising d orbitals and lower the strain and size mismatch in these alloys. Similar calculations show NiPd to be unstable and there is very little effect of relativity in these systems. The pair interaction calculations for these systems show NiPt have $L1_0$ as the stable ground state structure, as predicted from experiments. The positive value of the first-nearest neighbour pair energy in the NiPd system, even with the inclusion of relativistic effects, indicates that this alloy tends to order, but experimentally it seems to remain disordered to low temperatures.

Relativistic corrections ensure that the local magnetic moment of Ni is higher in NiPd than in NiPt, consistent with experiment. The low value of the local magnetic moment on the Ni site in NiPt is facilitated by relativistic corrections again through lowering of the s potential of Pt, which leads to a contraction of the s wavefunction and an increase in the s–d hybridization. We have obtained a Curie temperature for NiPt reasonably comparable to the experimental estimate. Our Curie temperature calculation including the short range segregation effect gives an enhancement in the Curie temperature in the NiPd system in better agreement with the experimental prediction than the calculation without it.

References

[1] Wang L G and Zunger A 2003 *Phys. Rev.* B **67** 092103
[2] Parra R E and Medina R 1980 *Phys. Rev.* B **22** 5460
[3] Cable J W and Child H R 1970 *Phys. Rev.* B **1** 3809
[4] Dahmani C E, Cadeville M C, Sanchez J M and Moran-Lopez J L 1985 *Phys. Rev. Lett.* **55** 1208
[5] Paudyal D, Saha-Dasgupta T and Mookerjee A 2004 *J. Phys.: Condens. Matter* **16** 2317
[6] Pinski F J, Staunton J B and Johnson D D 1998 *Phys. Rev.* B **57** 15177
[7] Ghosh S, Leath P L and Cohen M H 2002 *Phys. Rev.* B **66** 214206
[8] Saha T, Dasgupta I and Mookerjee A 1994 *J. Phys.: Condens. Matter* **6** 245
[9] Mookerjee A 1973 *J. Phys. C: Solid State Phys.* **6** 205
[10] von Barth U and Hedin L 1972 *J. Phys. C: Solid State Phys.* **5** 1629
[11] Andersen O K and Jepsen O 1984 *Phys. Rev. Lett.* **53** 2581
[12] Andersen O K, Jepsen O and Šob M 1987, 1992 *Electronic Band Structure and Its Applications* (*Springer Lecture Notes in Physics* vol 283) ed M Yussouff (Berlin: Springer)
[13] Andersen O K, Jespsen O and Krier G 1994 *Lectures on Methods of Electronic Structure Calculations* ed V Kumar, O K Andersen and A Mookerjee (Singapore: World Scientific)
[14] Das G P 2003 *Electronic Structure of Alloys, Surfaces and Clusters* (*Advances in Condensed Matter Science* vol 4) ed A Mookerjee and D D Sharma (London: Taylor and Francis)
[15] Heine V 1988 *Solid State Physics* vol 35 (New York: Academic)
[16] Paudyal D, Saha-Dasgupta T and Mookerjee A 2003 *J. Phys.: Condens. Matter* **15** 1029
[17] Kanamori J and Kakehasi Y 1977 *J Physique Coll.* **38** C7 274
[18] Mookerjee A and Prasad R 1993 *Phys. Rev.* B **48** 17724
[19] Saha T, Dasgupta I and Mookerjee A 1994 *Phys. Rev.* B **50** 13267
[20] Ghosh S, Chaudhuri C B, Sanyal B and Mookerjee A 2001 *J. Magn. Magn. Mater.* **234** 100
[21] Sanyal B, Biswas P P, Mookerjee A, Das G P, Salunke H and Bhattacharya A K 1998 *J. Phys.: Condens. Matter* **10** 5767

[22] Biswas P P, Sanyal B, Fakhruddin M, Halder A, Mookerjee A and Ahmed M 1995 *J. Phys.: Condens. Matter* **7** 8569
[23] Haydock R, Heine V and Kelly M J 1972 *J. Phys. C: Solid State Phys.* **5** 2845
[24] Kudrnovský J and Drchal V 1990 *Phys. Rev.* B **41** 7515
[25] Mohn P H and Wohlfarth E P 1987 *J. Phys. F: Met. Phys.* **17** 2421
[26] Gunnarson O 1976 *J. Phys. F: Met. Phys.* **6** 587
[27] Gersdorf R 1962 *J. Phys. Radium* **23** 726
[28] Ghosh S, Das N and Mookerjee A 1999 *J. Phys.: Condens. Matter* **9** 10701
[29] Ghosh S D 2000 *PhD Thesis* Jadavpur University